Chemosphere 279 (2021) 130631

Contents lists available at ScienceDirect

Chemosphere

journal homepage: www.elsevier.com/locate/chemosphere

Hg isotopic composition of one-year-old spruce shoots: Application to long-term Hg atmospheric monitoring in Germany

Akane Yamakawa [a, *], David Amouroux [b], Emmanuel Tessier [b], Sylvain Bérail [b], Ina Fettig [c], Julien P.G. Barre [d], Jan Koschorreck [c], Heinz Rüdel [e], Olivier F.X. Donard [b]

[a] National Institute for Environmental Studies, 16-2 Onogawa, Tsukuba, 305-8506, Japan
[b] Universite de Pau et des Pays de l'Adour, E2S UPPA, CNRS, IPREM, Institut des Sciences Analytiques et de Physico-chimie pour l'Environnement et les Matériaux. Technopôle Hélioparc, 2 Avenue Pierre Angot, 64053 Pau Cedex 09, France
[c] German Environment Agency (Umweltbundesamt), Corrensplatz 1, 14195, Berlin, Germany
[d] Advanced Isotopic Analysis, Technopôle Hélioparc Pau Pyrénées, 2 Avenue Pierre Angot, 64053 Pau Cedex 09, France
[e] Fraunhofer Institute for Molecular Biology and Applied Ecology IME, Auf dem Aberg 1, 57392, Schmallenberg, Germany

HIGHLIGHTS

- The shoots serve as passive samplers for airborne pollutants.
- Hg isotopic compositions of one-year-old spruce shoots were measured using CV-MC-ICP-MS.
- Δ^{199}Hg and Δ^{201}Hg did not significantly change during the study period.
- Δ^{200}Hg and δ^{202}Hg exhibited slight decreasing trends over time.
- Such decreases may be attributed to changes in the global and local Hg emissions.

ARTICLE INFO

Article history:
Received 6 February 2021
Received in revised form
5 April 2021
Accepted 18 April 2021
Available online 22 April 2021

Handling Editor: Lena Q. Ma

Keywords:
Mercury
Hg isotope
Biomonitoring
Atmospheric mercury
Spruce

ABSTRACT

The Hg isotopic composition of 1-year-old Norway spruce (*Picea abies*) shoots collected from Saarland cornurbation Warndt, Germany, since 1985 by the German Environmental Specimen Bank, were measured for a better understanding of the temporal trends of Hg sources. The isotopic data showed that Hg was mainly taken up as gaseous element mercury (GEM) and underwent oxidation in the spruce needles; this led to a significant decrease in the δ^{202}Hg compared with the atmospheric Hg isotopic composition observed for deciduous leaves and epiphytic lichens. Observation of the odd mass-independent isotopic fractionation (MIF) indicated that Δ^{199}Hg and Δ^{201}Hg were close to but slightly lower than the actual values recorded from the atmospheric measurement of the GEM isotopic composition in non-contaminated sites in U.S. and Europe, whereas observation of the even-MIF indicated almost no differences for Δ^{200}Hg. This confirmed that GEM is a major source of Hg accumulation in spruce shoots. Interestingly, the Hg isotopic composition in the spruce shoots did not change very significantly during the study period of >30 years, even as the Hg concentration decreased significantly. Even-MIF (Δ^{200}Hg) and mass-dependent fractionation (MDF) (δ^{202}Hg) of the Hg isotopes exhibited slight decrease with time, whereas odd-MIF did not show any clear trend. These results suggest a close link between the long-term evolution of GEM isotopic composition in the air and the isotopic composition of bioaccumulated Hg altered by mass-dependent fraction in the spruce shoots.

1. Introduction

Hg is a globally distributed toxic metal that is capable of long-distance transportation via the atmosphere and deposition on land. Atmospheric Hg exists as three chemical species, among which the dominant species (>90% of the total Hg in the lower atmosphere) is gaseous elemental mercury (GEM) or $Hg^0_{(g)}$. GEM has a relatively long atmospheric residence time (0.5–2 years), which allows regional and global transportation from emission

* Corresponding author.
E-mail address: yamakawa.akane@nies.go.jp (A. Yamakawa).

https://doi.org/10.1016/j.chemosphere.2021.130631

Table of abbreviations

GEM	Gaseous element mercury
GOM	Gaseous oxidized mercury
MDF	Mass-dependent fractionation
MIF	Mass-independent fractionation
PBM	Particulate-bound mercury
TGM	Total gaseous mercury

sources (Gonzalez-Raymat et al., 2017). The other two chemical species are gaseous oxidized mercury (GOM) or $Hg^{2+}_{(g)}$ and particulate-bound mercury (PBM) or $Hg_{(p)}$; they are relatively reactive and are efficiently removed from the atmosphere through wet and dry deposition (Lindberg et al., 2002; Liu et al., 2010). The global atmospheric Hg pool is fed not only by direct anthropogenic emissions (2000–3000 tonnes/year), but also by natural sources, primarily volcanic emissions (500 tonnes/year), and terrestrial re-emission of naturally and anthropogenically-derived Hg from soil and vegetation (1000 tonnes/year) and biomass burning (600 tonnes/year) (UNEP, 2019). Forest ecosystems are the largest sink for atmospheric Hg. Previous studies showed that leaves and tree rings can be used as biomonitors for total gaseous mercury (TGM, GEM + GOM) concentrations over space (Arnold et al., 2018; Peckham et al., 2019a, 2019b). GEM accumulates Hg in the foliage, primarily in stomata where it is retained in the oxidized form, and deposits with litterfall (Rutter et al., 2011). GOM and PBM are also adsorbed to leaf surfaces, and re-emitted to the atmosphere or leached by precipitation and deposited to the floor (Demers et al., 2007).

Despite the increased monitoring of atmospheric Hg, pollution detection and chronological records remain necessary for remote locations where continuous monitoring is difficult. Biomonitoring techniques are of great interest for evaluating concentration changes and possible sources of Hg. Particularly, conifers can serve as a bioindicator to determine the ambient air concentration and accumulation in plants during the time of exposure (Suchara et al., 2011; Kang et al., 2019; Liu et al., 2019). In the present study, spruce tree samples from a sampling site in the federal state Saarland, obtained from the German Environmental Specimen Bank (ESB), was used to obtain the trend of Hg isotopic composition with time, from 1985 to 2018. The German ESB is an organization of the German Federal Ministry for the Environment, Nature Conservation and Nuclear Safety for long-term monitoring of the environment and is technically and administratively managed by the Federal German Environment Agency. The German ESB systematically collects environmental samples from dedicated sampling regions and stores them to investigate spatial and temporal trends in pollution of the ecosystem by chemicals of emerging concern and/or to identify environmental threats early or the need for comprehensive environmental monitoring and regulatory risk management (Dreyer et al., 2019; Falk et al., 2019; Rüdel et al., 2010). Long-term storage of the sample occurs under cryogenic conditions, which prevents change in the state of chemical properties or loss of chemicals over several decades.

Hg has seven isotopes (196, 198, 199, 200, 201, 202, and 204) that can undergo mass-dependent fractionation (MDF) or mass-independent fractionation (MIF). Since the development of precise and accurate measurements, the stable isotopes of Hg can be analyzed to obtain information on its pollution sources and environmental pathways (Blum et al., 2014). MDF occurs during biogeochemical transformation, whereas odd-MIF (^{199}Hg and ^{201}Hg) occurs through a more complex mechanism mainly associated with photochemical processes. Previous studies have suggested that the global background atmospheric Hg pool is characterized by positive δ^{202}Hg values and urban-industrial emissions are characterized by more negative values (Demers et al., 2013; Gratz et al., 2010; Sherman et al., 2010; Yamakawa et al., 2017; Yu et al., 2016). Moreover, GOM and PBM generally show more positive MIF compared with that of GEM, which usually shows negative Δ^{199}Hg (Chen et al., 2012; Demers et al., 2013, 2015; Fu et al., 2014, 2016, 2018, 2019; Gratz et al., 2010; Sherman et al., 2012; Yamakawa et al., 2017, 2019, 2020; Yu et al., 2016; Zambardi et al., 2009). Investigations on the Hg isotopic composition in forest ecosystems (Barre et al., 2020; Demers et al., 2013; Yu et al., 2016; Yuan et al., 2019; Zheng et al., 2016) have shown that atmospheric gaseous Hg undergoes MDF during foliar uptake to generate lighter isotopes in plant leaves. Little MIF occurs in leaves, which indicates that the photochemical reactions of Hg are prevalent throughout the forest ecosystem (Demers et al., 2013).

This study aimed to (1) determine the temporal trends of Hg isotopic compositions in 1-year-old spruce shoots (*Picea abies*) for retrospective monitoring, (2) track sources of Hg, and (3) deepen understanding of the mechanisms underlying the biogeochemical Hg cycle in forest ecosystems. This unique dataset provides new information on the variability of the Hg isotopic composition in the atmosphere for the last few decades in Germany due to both local and global anthropogenic emissions.

2. Materials and methods

2.1. Sampling site, sample collection and pre-analysis of the sample

The sampling site, Warndt, Germany, is a natural forest located on the outer periphery of a densely populated and industrialized conurbation between the industrial regions of Saarland and Lorraine. The site is characterized by mixed stands of beech, oak, spruce, pine, and larch.

Spruce (*Picea abies*) samples (one-year shoots, each shoot consisting of needles, buds, and branch) are sampled each year from the crown of the tree (25–31 m above the ground), with the exception of the branch tip shoot. Each year the same standardized sampling protocol is used (Bartel et al., 2009). Samples are taken from the crowns of 15 trees at the same sampling site. Trees must be over 40 years old, predominant dominant or co-dominant in the stand. Immediately after sampling the shoots are rapid-frozen on-site in a Dewar vessel in the gas phase above liquid nitrogen and the cooling chain is not interrupted at any time afterwards. Thus transport, storage as well as grinding and homogenization of the sample material takes place under cryogenic conditions (temperature below approx. −130 °C) (Rüdel et al., 2015). Grinding and homogenizing is achieved using the cryo-oscillating mill KHD Humboldt Wedag Palla VM-KT with titanium milling cylinder and titanium milling rods (manufactured by KHD, Cologne) multiple times (Rüdel et al., 2008). The elemental concentrations of the spruce samples are reported in the open ESB database (www.umweltprobenbank.de/en/documents/investigations/). Total Hg concentrations were analyzed each year after short term storage (< 6 month) under cryogenic conditions (method: Rüdel et al., 2011). For this study all samples were analyzed again confirming these values, indicating that the samples were stored under stable conditions without any Hg loss. Fig. 1 shows that the Hg concentration in spruce has been gradually decreasing over time but had a peak around 2001; the Hg concentration was ~48 ng/g in 2001 and ~25 ng/g in 1999. Because the GEM concentration in Western Europe had no such peak (Zhang et al., 2016), this may indicate that the atmospheric Hg was due to local pollution. The inter-element correlation for spruce needles indicates strong correlations

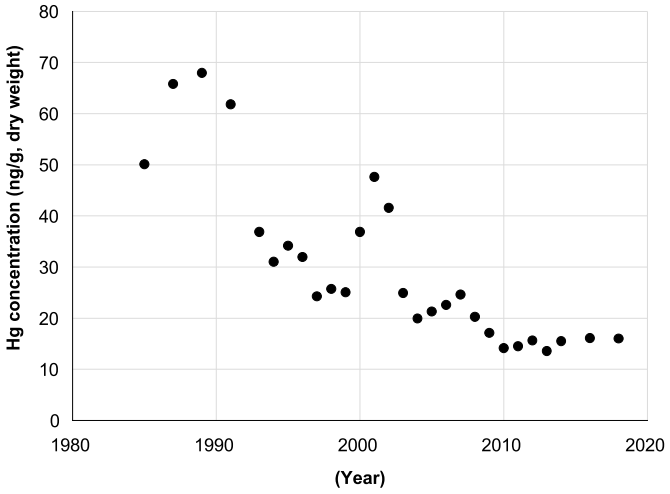

Fig. 1. Hg concentration of 1-year-old spruce (*Picea abies*) samples collected at Warnd, Germany.

between Hg and Cr, Fe, and Ni as well as significant correlations between Hg and Cu as well as Zn and Ba (Table S1).

2.2. Experimental methods

2.2.1. Reagents for Hg isotopic analysis

NIST SRM 3133 (Hg isotopic standard solution) was used as the primary standard, and NIST SRM 997 (Tl isotopic standard solution) was used to conduct an internal mass bias correction for the Hg isotope analysis. NIST RM 8610 (UM Almaden, Hg isotopic standard solution), BCR-482 (lichen), and NIST 1575a (pine needles) were used as secondary standards to ensure the quality of the analyses. Baker Instra-Analyzed Reagent (J. T. Baker, USA) was used to obtain HNO_3 for sample preparation and dilution. Ultrapure HNO_3 (Ultrex II grade, JT Baker, USA) was used to prepare the Tl solution. All pure water was prepared with a Milli-Q system (Merck Millipore, USA). Reagent-grade $SnCl_2 \cdot 2H_2O$ was obtained from Scharlau (Barcelona, Spain).

2.2.2. Sample preparation

An application note from Milestone for SRM NIST 1575a (pine needles) was referenced to dissolve the spruce samples. Approximately 0.5 g of the samples was decomposed by using 4 mL HNO_3 in a microwave (UltraWave, Milestone, Italy) at 230 °C for 25 min. To ensure analytical accuracy, the Hg isotopes of the secondary references (BCR-482 (lichen) and NIST 1575a (pine needles)) were measured with the same methods. The Hg concentrations of all dissolved samples were adjusted to 0.5 ppb.

2.2.3. Hg isotope analysis

Hg isotopic measurements were conducted with cold vapor multi-collector inductively coupled plasma mass spectrometry (CV-MC-ICP-MS) by using a Nu Plasma (Nu Instruments, UK) at IPREM (Institut des Sciences Analytiques et de Physicochimie pour l'Environnement et les Matériaux). Nu Plasma was interfaced with a DSN-100 desolvating nebulizer (Nu Instruments, UK) for Tl introduction and a homemade CV system for Hg^0 generation. Hg^0 and Tl dry aerosols (introduced Tl concentration: 15 μg/L) were mixed at the outlet of the CV generation system before being introduced into the plasma. The sample and standard solutions were diluted to appropriate Hg and acid concentrations (~10% HNO_3 and ~2% HCl, v/v), and Hg^{2+} was reduced online with 3% $SnCl_2$ in ~10% HCl. Hg and Tl isotopes were monitored simultaneously, and a $^{205}Tl/^{203}Tl$ isotope ratio of 2.38714 for NIST SRM 997 was used to correct for instrumental mass bias according to an exponential law.

In this study, the mass numbers of 198 (Hg), 199 (Hg), 200 (Hg), 201 (Hg), 202 (Hg), 203 (Tl), 204 (Hg, Pb), 205 (Tl), and 206 (Pb) were detected with individual Faraday cups. The preamplifier gains associated with each Faraday cup were calibrated daily. Instrumental parameters were tuned each day before the analysis to obtain the maximum signal intensity and stability. For each sample and standard, 30 cycles were collected with an integration time of 10 s for each cycle. Between sample analyses, the system was washed with 10% HNO_3 + 2% HCl to reduce the signal intensity for the CV system to the background level. The solution uptake rate was adjusted to 0.625 mL/min. The size of the bracketing standard was kept the same as that of the sample (0.5 ng/g). The typical intensity of ^{202}Hg was ~0.8 V. Signal intensities observed for the blank samples were typically less than 1% of those observed for the test samples. Blank subtractions were performed for each mass by using the on-peak zero method and running a blank solution (~10% HNO_3 and ~2% HCl, v/v) before each measurement. Table S2 presents the general settings.

The following raw isotopic ratios were corrected for instrumental mass bias by using the measured $^{205}Tl/^{203}Tl$ isotope ratios and its reference value (2.38714): $^{199}Hg/^{198}Hg$, $^{200}Hg/^{198}Hg$, $^{201}Hg/^{198}Hg$, $^{202}Hg/^{198}Hg$, and $^{204}Hg/^{198}Hg$. The uncertainty of these ratios was calculated by doubling the standard deviation (2SD) of the sample and bracketing the standard measurement mean (2σ). Any ratio with a value greater than 2SD was rejected.

Hg isotope ratios are generally reported as the actual ratios or δ values, which represent deviations in the isotope ratio from that of a standard in parts per thousand (per mil, denoted as ‰). All sample analyses were bracketed by analysis of an Hg isotopic standard solution (NIST SRM 3133), and Hg isotopic ratios were calculated relative to the mean of the bracketing standards (Blum and Bergquist, 2007):

$$\delta^{xxx}Hg\ (‰) = [(^{xxx}Hg/^{198}Hg)_{sample}/(^{xxx}Hg/^{198}Hg)_{NIST3133} - 1] \times 1000, \quad (1)$$

Where, ^{xxx} represents one of the five other possible isotopic mass numbers for Hg (199, 200, 201, 202, and 204).

In this study, MIF was reported by using Δ to indicate the difference between the measured $\delta^{xxx}Hg$ and theoretically predicted value of the same parameter according to the following relationship:

$$\Delta^{xxx}Hg\ (‰) = \delta^{xxx}Hg - \beta \times \delta^{202}Hg, \quad (2)$$

Where, β represents the equilibrium MDF factor, which is 0.252, 0.502, 0.752, and 1.493 for ^{199}Hg, ^{200}Hg, ^{201}Hg, and ^{204}Hg, respectively (Blum and Bergquist, 2007).

NIST RM 8610 (UM Almaden) was used as a secondary standard and was measured relative to NIST SRM 3133 several times for each analysis session. To determine the analytical uncertainty of an unknown sample, an external reproducibility of twice the standard error (2SE) is recommended for replicate analyses unless the external reproducibility of the method using the in-house secondary standard is less than 2SD (Blum and Bergquist, 2007). When 2SE of the sample replicates is less than the external reproducibility of the secondary standard, 2SD of the secondary standard should be reported as the uncertainty of the measured sample. In this study, the 2SD values of NIST RM 8610 (Table S3) were used to determine the analytical uncertainty of the measurements. The uncertainty attached to the Hg isotopic values was expanded by the coverage factor $k = 2$ corresponding to a confidence interval of approximately 95%. Type B uncertainty and uncertainty in the bias of the

methods were not included.

The repeatability of the Hg isotopic compositions for the secondary reference standard (NIST RM 8610), which were adjusted to 0.5 or 0.25 ng/g, was monitored during the study period to validate the analytical stability of the operating conditions (Table S3). Drifting of Hg isotopic ratios may occur during a daylong analysis as a consequence of Ar gas flow instability, cone and slit degradation, and/or cup aging. To overcome these potential problems, all sample analyses were bracketed according to the analytical results of the relevant standard (NIST SRM 3133), and the Hg isotopic values of a sample were calculated relative to the mean values of the corresponding parameters for the bracketing standard. With the standard-sample bracketing method, the deviations of the isotopic ratios measured for NIST RM 8610 were less than 0.3‰ ($n = 7$ and 9 for 0.5 and 0.25 ng/g, respectively) in the case of 0.5 and 0.25 ng/g solutions, and the results agreed with the published data (Estrade et al., 2010). BCR-482 and NIST 1575a, which have similar matrices to that of pine spruce, were also analyzed to validate and assure the analytical methods used for isotopic measurement and the sample decomposition. Our data are in good agreement with reference values (Estrade et al., 2010; Kurz et al., 2019). This result suggests that our methodology is sufficiently accurate to conduct Hg isotopic measurements. Table S3 reports the Hg isotopic compositions calculated for BCR-482 and NIST 1575a relative to the NIST SRM 3133 Hg standard. For the Hg isotopic measurements, BCR-482 was adjusted to 0.5 and 0.25 ng/g, and NIST 1575a was adjusted to 0.25 ng/g for Hg isotopic measurement. The measurements were all within an acceptable uncertainty to their counterparts in the literature (Estrade et al., 2010; Kurz et al., 2019). This result suggests that our technique is sufficient to measure.

3. Results and discussion

3.1. Hg concentration and isotopic composition in spruce needle shoots

The Hg concentration decreased rapidly from a peak of ~70 ng/g (dw) in 1989 (Fig. 1) to reach a background plateau of ~15 ng/g after 2010. The Hg isotopic composition of the spruce samples did not exhibit a large variation within the study period, even as the Hg concentration greatly decreased. The average Hg isotopic composition was $\delta^{202}Hg = -2.71 \pm 0.27‰$, $\Delta^{199}Hg = -0.41 \pm 0.13‰$, $\delta^{202}Hg = -0.01 \pm 0.08‰$, $\Delta^{201}Hg = -0.38 \pm 0.13‰$, and $\Delta^{204}Hg = 0.01 \pm 0.24‰$ (2SD, $n = 21$; see Table 1). Relatively small correlations between Hg concentration and sampling year and $\delta^{202}Hg$ and $\Delta^{200}Hg$ were observed. When we look through Hg concentration, $\Delta^{199}Hg$ and $\Delta^{201}Hg$ for the whole sampling year, we do not see any correlation between these two. On the other hand, there is significant correlation between Hg concentration and $\Delta^{199}Hg$ and $\Delta^{201}Hg$ for the sampling year from 2004 to 2018, with the small $\Delta^{199}Hg$ and $\Delta^{201}Hg$ peaks around 2004 (Fig. S1). MIF of odd-isotope is known to provide a unique fingerprint of specific chemical pathways, such as photochemical reduction. It may suggest that considerable evolution in emission sources and technologies might affect the isotopic composition during the years.

A negative $\delta^{202}Hg$ was observed, which may be caused during uptake by spruce. Forests are considered a net sink for atmospheric Hg because of the foliar uptake of GEM (e.g. Rutter et al., 2011; Jiskra et al., 2018). Foliar uptake followed by oxidation of GEM has been shown to induce significant MDF, and GEM may be oxidized by thiol ligands in foliar tissues (Demers et al., 2013). A slight positive correlation was observed between the MIF of the even isotope $\Delta^{200}Hg$ and the Hg concentration ($R^2 = 0.23$, $p = 0.03$) (Fig. 3(c)). Positive $\Delta^{200}Hg$ anomalies have been observed within precipitation that may originate from the upper atmosphere during GEM oxidation (Chen et al., 2012). Such anomalies in $\Delta^{200}Hg$ may derive from redox reactions that transform GEM into GOM, and the subsequent scavenging of GOM by droplets and particles (aerosols). Studies by Demers et al. (2013) and Jiskra et al. (2015) on remote forest ecosystems in the northern United States and Sweden suggest that GOM may only account for a small portion of atmospheric Hg deposition in forest soils, whereas the foliar uptake of GEM and the subsequent litterfall represent larger deposition pathways. The processes triggering $\Delta^{200}Hg$ have not been elucidated, but a plausible hypothesis is that photochemical oxidation of GEM in the atmosphere and mixing of different sources of GEM (i.e., pollution sources, soil evasion, and background atmosphere) result in the observed Hg isotopic composition for spruce. We also need to point out the contribution of PBM to the spruce samples. Since correlations between Hg and other heavy element are observed, a contribution from airborne particles, which adhered to the waxy cuticle, cannot be ruled out. However, in such background environment, even with Hg emission sources nearby, we do not expect large input from PBM (please see Barre et al., 2018 for evidence in lichens). In fact the Hg isotopic data shows no drastic change of MIF values along the years, implying that a major contribution of GEM is expected in the spruce shoots (at least in recent decades). However, we do not have Hg isotopic data of PBM at the sampling point, so that the contribution rate of Hg from PBM to spruce remains unknown.

3.2. Spatial and temporal trends for the Hg isotopic composition in spruce needles and other atmospheric biomonitors

In previous studies on remote forest ecosystems, the observed Hg isotope compositions in the forest soil and biomass differed from the isotopic composition of atmospheric Hg species (Demers et al., 2013; Enrico et al., 2016; Jiskra et al., 2015; Zhang et al., 2013; Zheng et al., 2016). These studies reported that the soil and forest biomass exhibited primarily negative odd-MIF ($\Delta^{199}Hg$ and $\Delta^{201}Hg$) with no significant even-MIF ($\Delta^{200}Hg$ and $\Delta^{204}Hg$), whereas atmospheric GOM samples predominantly show positive odd-MIF and even-MIF worldwide, and GEM shows a small degree of negative odd-MIF and even-MIF. The Hg isotopic composition of GEM from immediate anthropogenic emissions is characterized by negative $\delta^{202}Hg$ and near-zero $\Delta^{199}Hg$, whereas Hg associated with the regional background displays more positive $\delta^{202}Hg$ and negative $\Delta^{199}Hg$ (Demers et al., 2013; Gratz et al., 2010; Sherman et al., 2010; Yamakawa et al., 2017; Yu et al., 2016).

Fig. 4 compares the Hg isotopic compositions of the spruce samples in this study and foliage samples collected at non-contaminated sites in the United States and Europe. Demers et al. (2013) measured the Hg isotopic compositions of precipitation and TGM/GEM and showed that $\Delta^{199}Hg$ significantly differed for foliage and precipitation samples. This result implies that precipitation is not the source of Hg in foliage. The $\delta^{202}Hg$ values for the spruce (−2.95‰ to −2.40‰, $n = 21$) were slightly lower than those of foliage in US forests, although there was some overlap (−2.53‰ to −1.79‰, $n = 19$, Demers et al., 2013; −2.67‰ to −2.08‰, $n = 9$, Zheng et al., 2016). The $\Delta^{199}Hg$ and $\Delta^{200}Hg$ values for the spruce were similar to those reported by Demers et al. (2013) ($\Delta^{199}Hg$: from −0.40‰ to −0.22‰, $\Delta^{200}Hg$: from −0.13‰ to 0.16‰) and Zheng et al. (2016) ($\Delta^{199}Hg$: from −0.47‰ to −0.06‰, $\Delta^{200}Hg$: from −0.04‰ to 0.04‰). Despite the different tree species and geographic areas, Hg in vegetation may mainly derive from similar sources, such as the global (or northern hemispheric) background GEM, and/or undergoes similar fractionation mechanisms. Additionally, Barre et al. (2020) recently studied Hg isotopes in epiphytic lichens in a large and remote beech forested area at the French–Spanish border. They found a wider range but similar average for $\delta^{202}Hg$ (from −4.69‰ to −1.71‰,

Table 1
Hg isotopic concentrations and compositions of 1-year-old spruce shoots.

Sampled year	Hg ppb (dw)	1/Hg	δ^{199}Hg	δ^{200}Hg	δ^{201}Hg	δ^{202}Hg	δ^{204}Hg	Δ^{199}Hg	Δ^{200}Hg	Δ^{201}Hg	Δ^{204}Hg
			‰	‰	‰	‰	‰	‰	‰	‰	‰
1985	50.100	0.020	−1.06	−1.26	−2.38	−2.61	−4.04	−0.40	0.05	−0.42	−0.15
1987	65.820	0.015	−0.98	−1.13	−2.20	−2.40	−3.80	−0.38	0.08	−0.39	−0.22
1989	67.960	0.015	−1.05	−1.32	−2.35	−2.59	−4.06	−0.40	−0.03	−0.41	−0.20
1993	36.883	0.027	−0.97	−1.28	−2.28	−2.63	−4.01	−0.30	0.04	−0.30	−0.08
1995	34.183	0.029	−1.15	−1.31	−2.31	−2.53	−3.64	−0.51	−0.04	−0.40	0.15
1995	34.183	0.029	−1.18	−1.47	−2.47	−2.82	−4.04	−0.47	−0.05	−0.35	0.17
1995	34.183	0.029	−1.03	−1.35	−2.41	−2.63	−3.77	−0.36	−0.03	−0.43	0.16
1997	24.283	0.041	−1.02	−1.38	−2.37	−2.70	−4.04	−0.34	−0.02	−0.34	−0.01
1999	25.050	0.040	−1.24	−1.52	−2.49	−2.95	−4.35	−0.50	−0.04	−0.28	0.05
2000	36.883	0.027	−1.12	−1.35	−2.42	−2.75	−3.96	−0.43	0.03	−0.36	0.14
2001	47.617	0.021	−1.15	−1.39	−2.45	−2.70	−4.15	−0.47	−0.03	−0.43	−0.12
2002	41.583	0.024	−1.07	−1.36	−2.39	−2.72	−4.19	−0.39	0.01	−0.35	−0.14
2003	24.917	0.040	−1.16	−1.40	−2.49	−2.81	−4.16	−0.46	0.01	−0.38	0.03
2004	19.933	0.050	−1.16	−1.42	−2.61	−2.83	−4.19	−0.44	0.01	−0.48	0.03
2006	22.600	0.044	−1.19	−1.40	−2.62	−2.82	−4.19	−0.48	0.02	−0.51	0.01
2008	20.283	0.049	−1.14	−1.35	−2.45	−2.69	−4.01	−0.47	0.00	−0.43	0.00
2010	14.150	0.071	−1.14	−1.49	−2.50	−2.83	−4.18	−0.43	−0.07	−0.37	0.05
2012	15.633	0.064	−1.09	−1.58	−2.48	−2.92	−4.35	−0.35	−0.11	−0.28	0.01
2014	15.525	0.064	−0.92	−1.34	−2.25	−2.64	−3.87	−0.26	−0.01	−0.27	0.07
2016	16.100	0.062	−1.08	−1.43	−2.54	−2.81	−4.20	−0.37	−0.02	−0.42	0.01
2018	16.025	0.062	−1.13	−1.37	−2.39	−2.66	−3.76	−0.46	−0.03	−0.39	0.20
Average			−1.10	−1.37	−2.42	−2.71	−4.05	−0.41	−0.01	−0.38	0.01
2SD ($n = 21$)			0.16	0.19	0.22	0.27	0.39	0.13	0.08	0.13	0.24

Expanded uncertainties (2SD) of spruce taken from NIST RM 8610.

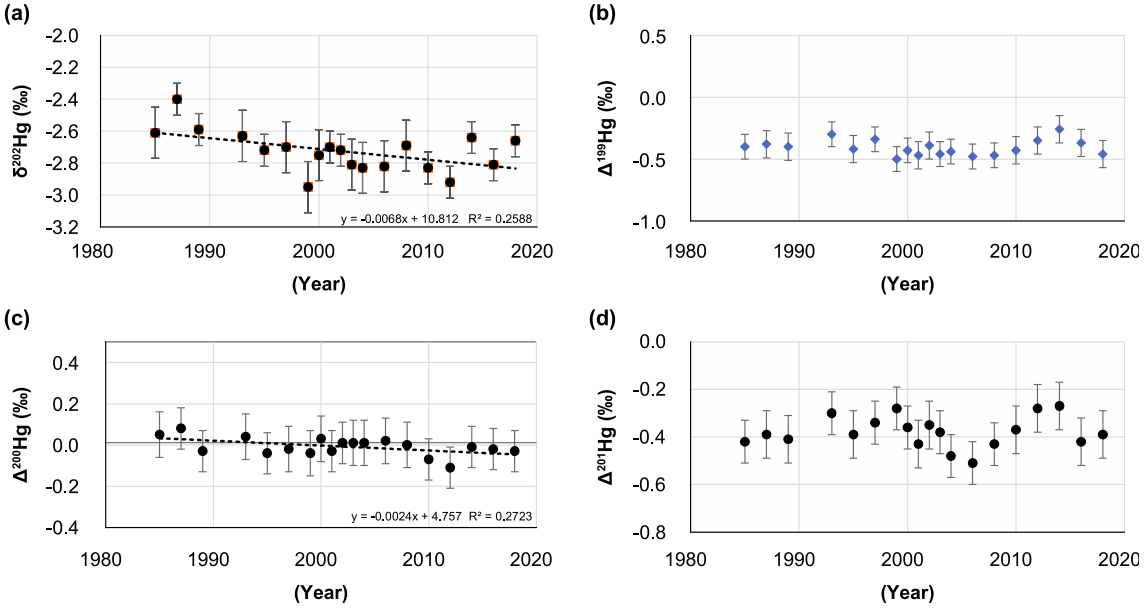

Fig. 2. Temporal variations of (a) δ^{202}Hg, (b) Δ^{199}Hg, (c) Δ^{200}Hg, and (d) Δ^{201}Hg in spruce. The uncertainties of each plot represent 2SD of NIST RM 8610 as reported in Table S3.

average: −2.68 ± 1.55‰, $n = 58$) and Δ^{200}Hg (from −0.07‰ to 0.13‰, average: 0.01 ± 0.07‰, $n = 58$) and slightly less negative values for Δ^{199}Hg (from −0.47‰ to 0.03‰, average: −0.19 ± 0.26‰, $n = 58$). Such a difference for odd-MIF may be explained by larger photoreduction pathways for spruce shoots compared to lichens, which are located below the tree canopy.

3.3. Long-term trend of Hg isotopic composition derived from ambient GEM uptake

The isotopic composition was consistent throughout the sampling period (1985–2018), which indicates that the vegetation was mostly taking up atmospheric GEM. Nevertheless, specific trends were observed for both δ^{202}Hg (MDF) and Δ^{200}Hg (even-MIF), which exhibited a steady decrease. δ^{202}Hg and Δ^{200}Hg followed linear decreasing trends with $R^2 = 0.26$ ($p = 0.02$) and $R^2 = 0.27$ ($p = 0.03$), respectively. Whether such trends are statistically significant remains difficult to ascertain because of the inherent uncertainties associated with both isotopic signatures (2SD). By contrast, no specific trends could be observed for odd-MIF (^{199}Hg and ^{201}Hg). However, the values of Δ^{199}Hg/Δ^{201}Hg were plotted along a slope of ~1 together with other studies on lichen and foliage samples from non-polluted sites (Fig. 5). This suggests photochemical and gas exchange processes at the needle shoot surface (i.e., GEM<=>GOM exchange).. Strongly negative δ^{202}Hg was observed, which may be caused during uptake by the spruce.

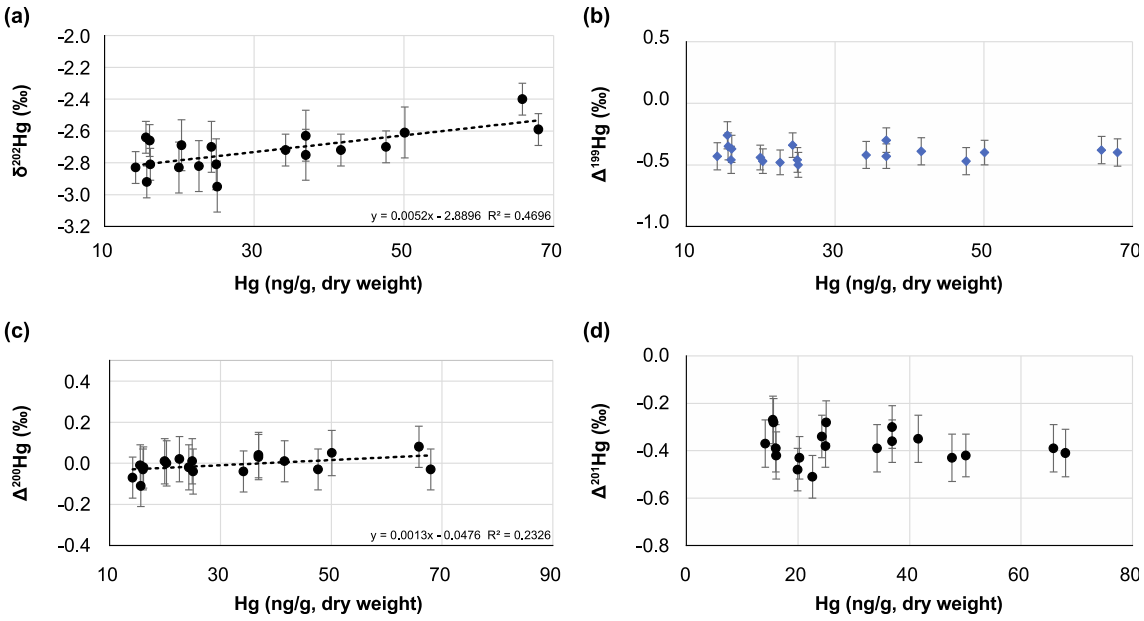

Fig. 3. Hg concentration vs. (a) δ^{202}Hg, (b) Δ^{199}Hg, (c) Δ^{200}Hg, and (d) Δ^{201}Hg in spruce. Uncertainties of each plot represent 2SD of NIST RM 8610 as reported in Table S3.

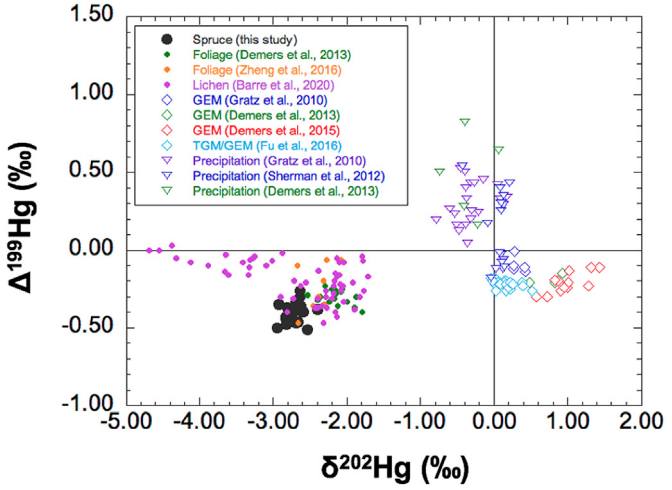

Fig. 4. δ^{202}Hg vs. Δ^{199}Hg for spruce samples in this study compared with those for foliage, lichen, GEM, and precipitation samples in the literature.

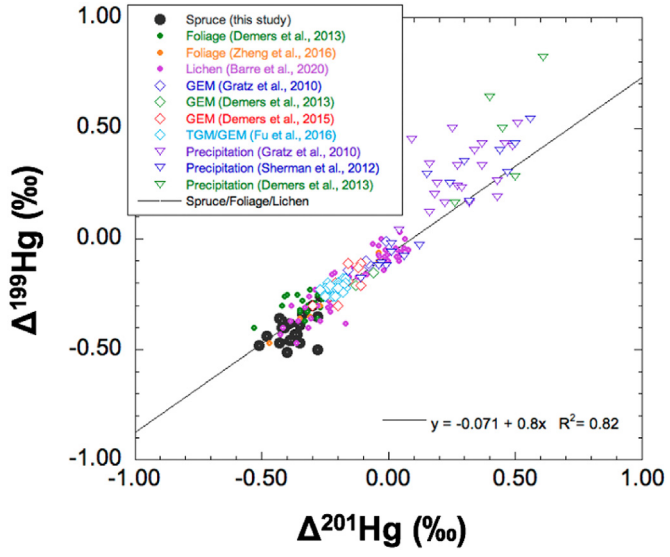

Fig. 5. Δ^{201}Hg vs. Δ^{199}Hg for spruce samples in this study compared with those for foliage, lichen, GEM, and precipitation samples in the literature.

Although such a process erases the original information on the pollution sources, the large MDF during TGM uptake may be essential for understanding the isotopic balance of the global mercury cycle. However, the local emissions have changed noteworthy, especially in the surrounding area of the sampling site. In the last 30–40 years, large industrial and metallurgical facilities have mostly collapsed or evolved to cleaner technologies, which has been related to modernizations in the steel industry and the close-down of the old coke oven in the near-by Völklingen industrial region (explained in www.umweltprobenbank.de/en/documents/selected_results/13061). Generally, mercury emissions in Germany declined by approximately 77% since the 1990s until 2018 (European Environment Agency, 2020). The results of this study established that such large changes in local Hg emissions did not induce drastic variations in the Hg isotopic composition of the air (gas phase) and subsequently in the vegetation.

4. Conclusion

The Hg isotopic composition in 1-year-old shoots of Norway spruce shoots collected since 1985 in Germany was measured by using CV-MC-ICP-MS. Although the Hg concentration decreased significantly over time until late 2010, the Hg isotopic composition did not significantly change during the sampling period. The reason that there is no significant trend of Hg isotopes in spruce shoots is that the main atmospheric process might be constant at the sampling area. However, a small even-MIF (Δ^{200}Hg) shift that should not change after uptake is observed. Even-MIF (Δ^{200}Hg) and MDF (δ^{202}Hg) for the Hg isotopic composition both exhibited slight decreasing trends over time. Such decreases may be attributed to changes in the global and local Hg emissions (European Environment Agency, 2020) and in the contribution of the

atmosphere to the deposition of Hg species (GEM, GOM, and wet deposition). Environmental samples like spruce shoots can be used as passive monitoring samples or bioindicators for measurement of Hg isotopic signature to reveal past and present information about atmospheric Hg deposition, fate, and origin, especially at the polluted region. Further investigations of the atmospheric Hg cycle of the area are necessary (such as GEM/GOM/PBM monitoring, and Hg isotopic measurements of GEM/GOM/PBM, tree rings, and environmental samples nearby).

Data availability

All elemental concentration data can be accessed via the German Environmental Specimen Bank website at https://www.umweltprobenbank.de/en/documents (last access: Apr. 14, 2020).

Author contributions

A.Y., E.T., S.B., J.B., and H.R. performed the experiments and the analysis. A.Y., D.A., I.F., and J.K. designed the figures and wrote the original draft. O.D. and D.A. supervised the project.

Funding

This research is part of the project MercOx and is funded by the European Metrology Program for Innovation and Research program co-financed by the Participating States and by the European Union's Horizon 2020 research and innovation program (EMPIR EURAMET, Grant number 16ENV01).

Declaration of competing interest

The authors declare that they have no known competing financial interests or personal relationships that could have appeared to influence the work reported in this paper.

Acknowledgment

We thank Heinz Rüdel and his group for the sample preparation and measurement of Hg in the spruce shoots. We want to thank the anonymous reviewers and editor for their valuable and constructive comments that significantly contributed to the manuscript. The authors would like to thank Enago (www.enago.jp) for the English language review.

Appendix B. Supplementary data

Supplementary data to this article can be found online at https://doi.org/10.1016/j.chemosphere.2021.130631.

Ethical considerations

We have used spruce shoots for this study. Hence, ethics committee approval, informed consent etc. is not applicable.

References

Arnold, J., Gustin, M.S., Weisberg, P.J., 2018. Evidence for nonstomatal uptake of Hg by aspen and translocation of Hg from foliage to tree rings in Austrian pine. Environ. Sci. Technol. 52 (3), 1174–1182. https://doi.org/10.1021/acs.est.7b0446.

Barre, J.P.G., Queipo-Abad, S., Sola-Larrañaga, C., Deletraz, G., Bérail, S., Tessier, E., Elustondo Valencia, D., Santamaría, J.M., de Diego, A., Amouroux, D., 2020. Comparison of the isotopic composition of Hg and Pb in two atmospheric bioaccumulators in a Pyrenean beech forest (Iraty Forest, Western Pyrenees, France/Spain). Front. Environ. Chem. 1, 582001. https://doi.org/10.3389/fenvc.2020.582001.

Bartel, M., Klein, R., Paulus, M., Tarricone, M.Q.K., Teubner, D., Wagner, G.. Guidelines for sampling, transport, storage and chemical characterization of environmental and human samples. Version 2.0.1. July 2009, fraunhofer IME, schmallenberg, Germany and German environment agency. https://www.umweltprobenbank.de/upb_static/fck/download/SOP_Spruce_Pine_V2.0.1_2009_en.pdf.

Blum, J.D., Sherman, L.S., Johnson, M.W., 2014. Mercury isotopes in earth and environmental sciences. Annu. Rev. Earth Planet Sci. 42, 249–269. https://doi.org/10.1146/annurev-earth-050212-124107.

Blum, J.D., Bergquist, B.A., 2007. Reporting of variations in the natural isotopic composition of mercury. Anal. Bioanal. Chem. 388, 353–359. https://doi.org/10.1007/s00216-007-1236-9.

Chen, J., Hintelmann, H., Feng, X., Dimock, B., 2012. Unusual fractionation of both odd and even mercury isotopes in precipitation from Peterborough, ON, Canada. Geochem. Cosmochim. Acta 90, 33–46. https://doi.org/10.1016/j.gca.2012.05.005.

Demers, J.D., Driscoll, C.T., Fahey, T.J., Yavitt, J.B., 2007. Mercury cycling in litter and soil in different forest types in the Adirondack region, New York, USA. Ecol. Appl. 17, 1341–1351. https://doi.org/10.1890/06-1697.1.

Demers, J.D., Blum, J.D., Zak, D.R., 2013. Mercury isotopes in a forested ecosystem: implications for air-surface exchange dynamics and the global mercury cycle. Global Biogeochem. Cycles 27, 222–238. https://doi.org/10.1002/gbc.20021.

Demers, J.D., Sherman, L.S., Blum, J.D., Marsik, F.J., Dvonch, J.T., 2015. Coupling atmospheric mercury isotope ratios and meteorology to identify sources of mercury impacting a coastal urban-industrial region near Pensacola. Global Biogeochem. Cycles 29, 1689–1705. https://doi.org/10.1002/2015gb005146.

Dreyer, A., Neugebauer, F., Lohmann, N., Rüdel, H., Teubner, D., Grotti, M., Rauert, C., Koschorreck, J., 2019. Recent findings of halogenated flame retardants (HFR) in the German and Polar environment. Environ. Pollut. 253, 850–863. https://doi.org/10.1016/j.envpol.2019.07.070.

Enrico, M., Roux, G.L., Marusczak, N., Heimbürger, L.E., Claustres, A., Fu, X., Sun, R., Sonke, J.E., 2016. Atmospheric mercury transfer to peat bogs dominated by gaseous elemental mercury dry deposition. Environ. Sci. Technol. 50, 2405–2412. https://doi.org/10.1021/acs.est.5b06058.

Estrade, N., Carignan, J., Donard, O.F.X., 2010. Isotope tracing of atmospheric mercury sources in an urban area of northeastern France. Environ. Sci. Technol. 44, 6062–6067. https://doi.org/10.1021/es100674a.

European Environment Agency, 2020. European Union emission inventory report 1990-2018, Under the UNECE Convention on Long-range Transboundary Air Pollution (LRTAP). European Environment Agency, 2020, Luxembourg. https://www.eea.europa.eu/publications/european-union-emission-inventory-report-1990-2018. (Accessed 23 April 2021). EEA Report No 5/2020.

Falk, S., Stahl, T., Fliedner, A., Rüdel, H., Tarricone, K., Brunn, H., Koschorreck, J., 2019. Levels, accumulation patterns and retrospective trends of perfluoroalkyl acids (PFAAs) in terrestrial ecosystems over the last three decades. Environ. Pollut. 246, 921–931. https://doi.org/10.1016/j.envpol.2018.12.095.

Fu, X., Heimbürger, L.-E., Sonke, J.E., 2014. Collection of atmospheric gaseous mercury for stable isotope analysis using iodine- and chlorine-impregnated activated carbon traps. J. Anal. At. Spectrom. 29, 841–852. https://doi.org/10.1039/c3ja50356a.

Fu, X., Marusczak, N., Wang, X., Gheusi, F., Sonke, J.E., 2016. Isotopic composition of gaseous elemental mercury in the free troposphere of the pic du midi observatory, France. Environ. Sci. Technol. 50, 5641–5650. https://doi.org/10.1021/acs.est.6b00033.

Fu, X., Yang, X., Tan, Q., Ming, L., Lin, T., Lin, C.-J., Li, X., Feng, X., 2018. Isotopic composition of gaseous elemental mercury in the marine boundary layer of East China sea. J. Geophys. Res. Atmos. 7656–7669. https://doi.org/10.1029/2018jd028671.

Fu, X., Zhang, H., Feng, X., Tan, Q., Ming, L., Liu, C., Zhang, L., 2019. Domestic and transboundary sources of atmospheric particulate bound mercury in remote areas of China: evidence from mercury isotopes. Environ. Sci. Technol. 53, 1947–1957. https://doi.org/10.1021/acs.est.8b06736.

Gratz, L.E., Keeler, G.J., Blum, J.D., Sherman, L.S., 2010. Isotopic composition and fractionation of mercury in great lakes precipitation and ambient air. Environ. Sci. Technol. 44, 7764–7770. https://doi.org/10.1021/es100383w.

Jiskra, M., Sonke, J.E., Obrist, D., Bieser, J., Ebinghaus, R., Myhre, C.L., Pfaffhuber, K.A., Wängberg, I., Kyllönen, K., Worthy, D., Martin, L.G., Labuschagne, C., Mkololo, T., Ramonet, M., Magand, O., Dommergue, A., 2018. A vegetation control on seasonal variations in global atmospheric mercury concentrations. Nat. Geosci. 11, 244–250. https://doi.org/10.1038/s41561-018-0078-8.

Jiskra, M., Wiederhold, J.G., Skyllberg, U., Kronberg, R.-M., Hajdas, I., Kretzschmar, R., 2015. Mercury deposition and re-emission pathways in boreal forest soils investigated with Hg isotope signatures. Environ. Sci. Technol. 49, 7188–7196. https://doi.org/10.1021/acs.est.5b00742, 2015.

Kang, H., Liu, X., Guo, J., Wang, B., Xu, G., Wu, G., Kang, S., Huang, J., 2019. Characterization of mercury concentration from soils to needle and tree rings of Schrenk spruce (Picea schrenkiana) of the middle Tianshan Mountains, northwestern China. Ecol. Indicat. 104, 24–31. https://doi.org/10.1016/j.ecolind.2019.04.066.

Kurz, A.Y., Blum, J.D., Washburn, S.J., Baskaran, M., 2019. Changes in the mercury isotopic composition of sediments from a remote alpine lake in Wyoming, USA. Sci. Total Environ. 669, 973–982. https://doi.org/10.1016/j.scitotenv.2019.03.165.

Lindberg, S.E., Brooks, S., Lin, C.-J., Scott, K.J., Landis, M.S., Stevens, R.K., Goodsite, M., Richter, A., 2002. Dynamic oxidation of gaseous mercury in the Arctic troposphere at polar sunrise. Environ. Sci. Technol. 36, 1245–1256. https://doi.org/

10.1021/es0111941.
Liu, B., Keeler, G.J., Dvonch, T., Barres, J.A., Lynam, M.M., Marsik, F.J., Morgan, J.T., 2010. Urban–rural differences in atmospheric mercury speciation. Atmos. Environ. 44, 2013–2023. https://doi.org/10.1016/j.atmosenv.2010.02.012.
Liu, H.W., Shao, J.J., Yu, B., Liang, Y., Duo, B., Fu, J.J., Yang, R.Q., Shi, J.B., Jiang, G.B., 2019. Mercury isotopic compositions of mosses, conifer needles, and surface soils: implications for mercury distribution and sources in Shergyla Mountain, Tibetan Plateau. Ecotoxicol. Environ. Saf. 172, 225–231. https://doi.org/10.1016/j.ecoenv.2019.01.082.
Peckham, M.A., Gustin, M.S., Weisberg, P.J., 2019a. Assessment of the suitability of tree rings as archives of global and regional atmospheric mercury pollution. Environ. Sci. Technol. 53 (7), 3663–3671. https://doi.org/10.1021/acs.est.8b06786.
Peckham, M.A., Gustin, M.S., Weisberg, P.J., Weiss-Penzias, P., 2019b. Results of a controlled field experiment to assess the use of tree tissue concentrations as bioindicators of air Hg. Biogeochemistry 142, 265–279. https://doi.org/10.1007/s10533-018-0533-z.
Rüdel, H., Uhlig, S., Weingärtner, M., December 2008. Pulverisation and Homogenisation of Environmental Samples by Cryomilling. Guidelines for Sampling and Sample Processing. Fraunhofer IME, Schmallenberg, Germany and German Environment Agency, Dessau-Rosslau, Germany, Version 2.0.0. https://www.umweltprobenbank.de/upb_static/fck/download/IME_SOP_Probenvorbereitung_Dez2008_V200.pdf.
Rüdel, H., Fliedner, A., Kösters, J., Schröter-Kermani, C., 2010. Twenty years of elemental analysis of marine biota within the German Environmental Specimen Bank—a thorough look at the data. Environ. Sci. Pollut. Res. 17, 1025–1034. https://doi.org/10.1007/s11356-009-0280-8.
Rüdel, H., Kösters, J., Schörmann, J., 2011. Guidelines for chemical analysis: determination of the elemental content of environmental samples using ICP-MS. http://www.umweltprobenbank.de/en/documents/publications/15168.
Rüdel, H., Weingärtner, M., Klein, R., Deutsch, A., 2015. Guidelines for sampling and sample processing: transporting environmental samples under cryogenic conditions. Fraunhofer IME, schmallenberg, and university of trier. https://www.umweltprobenbank.de/upb_static/fck/download/SOP_Transport_EN.pdf.
Rutter, A.P., Schauer, J.J., Shafer, M.M., Creswell, J.E., Olson, M.R., Robinson, M., Collins, R.M., Parman, A.M., Katzman, T.L., Mallek, J.L., 2011. Dry deposition of gaseous elemental mercury to plants and soils using mercury stable isotopes in a controlled environment. Atmos. Environ. 45, 848–855. https://doi.org/10.1016/j.atmosenv.2010.11.025.
Sherman, L.S., Blum, J.D., Keeler, G.J., Demers, J.D., Dvonch, J.T., 2012. Investigation of local mercury deposition from a coal-fired power plant using mercury isotopes. Environ. Sci. Technol. 46, 382–390. https://doi.org/10.1021/es202793c.
Sherman, L.S., Blum, J.D., Johnson, K.P., Keeler, G.J., Barres, J.A., Douglas, T.A., 2010. Mass-independent fractionation of mercury isotopes in Arctic snow driven by sunlight. Nat. Geosci. 3, 173–177. https://doi.org/10.1038/ngeo758.
Suchara, I., Sucharova, J., Hola, M., Reimann, C., Boyd, R., Filzmoser, P., Englmaier, P., 2011. The performance of moss, grass, and 1- and 2-year old spruce needles as bioindicators of contamination: a comparative study at the scale of the Czech Republic. Sci. Total Environ. 409, 2281–2297. https://doi.org/10.1016/j.scitotenv.2011.02.003.
UNEP, 2019. Global 3ercury Assessment. Sources, Emissions, Releases and Environmental Transport. UNEP Chemicals and Health Branch, Geneva, Switzerland, ISBN 978-92-807-3744-8, p. 2018.
Yamakawa, A., Moriya, K., Yoshinaga, J., 2017. Determination of isotopic composition of atmospheric mercury in urban-industrial and coastal regions of Chiba, Japan, using cold vapor multicollector inductively coupled plasma mass spectrometry. Chem. Geol. 448, 84–92. https://doi.org/10.1016/j.chemgeo.2016.11.010.
Yamakawa, A., Takami, A., Takeda, Y., Kato, S., Kajii, Y., 2019. Emerging investigator series: investigation of mercury emission sources using Hg isotopic compositions of atmospheric mercury at the Cape Hedo Atmosphere and Aerosol Monitoring Station (CHAAMS), Japan. Environ. Sci. Process. Impacts. 21, 809–818. https://doi.org/10.1039/c8em00590g.
Yamakawa, A., Bérail, S., Amouroux, D., Tessier, E., Barre, J., Sano, T., Nagano, K., Kanwal, S., Yoshinaga, J., Donard, O.F.X., 2020. Hg isotopic composition and total Hg mass fraction in NIES Certified Reference Material No. 28 Urban Aerosols. Anal. Bioanal. Chem. 412, 4483–4493. https://doi.org/10.1007/s00216-020-02691-9.
Yu, B., Fu, X., Yin, R., Zhang, H., Wang, X., Lin, C.J., Wu, C., Zhang, Y., He, N., Fu, P., Wang, Z., Shang, L., Sommar, J., Sonke, J.E., Maurice, L., Guinot, B., Feng, X., 2016. Isotopic composition of atmospheric mercury in China: new evidence for sources and transformation processes in air and in vegetation. Environ. Sci. Technol. 50, 9262–9269. https://doi.org/10.1021/acs.est.6b01782.
Yuan, W., Sommar, J., Lin, C.-J., Wang, X., Li, K., Liu, Y., Zhang, H., Lu, Z., Wu, C., Feng, X., 2019. Stable isotope evidence shows re-emission of elemental mercury vapor occurring after reductive loss from foliage. Environ. Sci. Technol. 53, 651–660. https://doi.org/10.1021/acs.est.8b04865.
Zambardi, T., Sonke, J.E., Toutain, J.P., Sortino, F., Shinohara, H., 2009. Mercury emissions and stable isotopic compositions at Vulcano Island (Italy). Earth Planet Sci. Lett. 277, 236–243. https://doi.org/10.1016/j.epsl.2008.10.023.
Zhang, H., Yin, R.S., Feng, X.B., Sommar, J., Anderson, C.W.N., Sapkota, A., Fu, X.-w., Larssen, T., 2013. Atmospheric mercury inputs in montane soils increase with elevation: evidence from mercury isotope signatures. Sci. Rep. 3 (3322), 1–8. https://doi.org/10.1038/srep03322.
Zhang, Y., Jacob, D.J., Horowitz, H.M., Chen, L., Amos, H.M., Krabbenhoft, D.P., Slemr, F., St Louis, V.L., Sunderland, E.M., 2016. Observed decrease in atmospheric mercury explained by global decline in anthropogenic emissions. Proc. Natl. Acad. Sci. U. S. A. 113, 526–531. https://doi.org/10.1073/pnas.1516312113.
Zheng, W., Obrist, D., Weis, D., Bergquist, B.A., 2016. Mercury isotope compositions across North American forests. Global Biogeochem. Cycles 30, 1475–1492. https://doi.org/10.1002/2015GB005323.